Dependence of the Jahn-Teller distortion in $LaMn_{1-x}Sc_xO_3$ on the isovalent Mn-site substitution

G Subías[1], V Cuartero[2], J Blasco[1], J García[1], C Meneghini[3] and G Aquilanti[4]

[1]Instituto de Ciencia de Materiales de Aragón, Departamento de Física de la Materia Condensada, CSIC-Universidad de Zaragoza, C/ Pedro Cerbuna 12, 50009 Zaragoza (Spain)
[2]ESRF-The European Synchrotron, 71, Avenue des Martyrs, Grenoble (France)
[3]Dipartimento di Scienze, Università Roma TRE, Via della Vasca Navale 84 – 00146, Roma, (Italy)
[4]Elettra-Sincrottrone Trieste, S.S. 14, Km 163.5, 34149 Basovizza, Trieste (Italy)

E-mail: gloria@unizar.es

Abstract. We investigated the relative importance of removing the Mn^{3+} Jahn-Teller distortion in driving ferromagnetism in $LaMn_{1-x}Sc_xO_3$ combining x-ray powder diffraction and x-ray absorption spectroscopy at the Mn and Sc K-edges. By increasing the Sc content, the orthorhombic distortion of the *Pbnm* cell in $LaMnO_3$ decreases but the unit-cell remains slightly distorted in $LaScO_3$. Besides, the nearly tetragonal-distorted MO_6 in $LaMnO_3$ continuously evolves into a nearly regular one in $LaScO_3$. On the other hand, x-ray absorption spectra show that the MnO_6 octahedron remains Jahn-Teller distorted and the ScO_6 octahedron is nearly regular along the whole series. Moreover, the ordering of the Mn^{3+} Jahn-Teller distortion is not disrupted in the ab plane for any Sc concentration. This contrasts with the Ga-substituted compounds, where a regular MnO_6 is found for x>0.5. However, both $LaMn_{0.5}Sc_{0.5}O_3$ and $LaMn_{0.5}Ga_{0.5}O_3$ show ferromagnetic behavior independently of the presence (or not) of Jahn-Teller distorted Mn^{3+}. Thus, our results point to the Mn-sublattice dilution as the main effect in driving ferromagnetism in these manganites over local structure effects previously proposed by the spin flipping or the vibronic superexchange models.

1. Introduction

Doped manganites have been extensively studied owing to their colossal magnetoresistance property and its potential applications to magnetic devices. In particular, $LaMnO_3$ is considered as the prototype of the cooperative Jahn-Teller (JT) systems and orbital-ordered state [1]. It also develops long-range antiferromagnetic (AFM) ordering of type A below T_N=140 K. The substitution at the Mn dramatically modifies the magnetic and electronic properties. It is known that the A-type AFM orbitally ordered state of $LaMnO_3$ is easy destroyed to give way to ferromagnetism (FM) by introducing various cations on the Mn site [2-5]. However, this ferromagnetic behavior derives from a complex interplay between several mechanisms: double-exchange and super-exchange interactions, orbital order and JT distortions. The substitution of Mn with non-magnetic isovalent ions such as Ga^{3+} ($3d^{10}$) or Sc^{3+} ($3d^0$) weakens the Mn^{3+}-Mn^{3+} super-exchange interactions but surprisingly favors the appearance of a FM ground state for $LaMn_{0.5}Ga_{0.5}O_3$ [3,4] and $LaMn_{0.5}Sc_{0.5}O_3$ [5]. Two models have been reported to account for this property: the spin flipping of Mn e_g-orbital in JT-distorted Mn^{3+} atoms surrounded by

Content from this work may be used under the terms of the Creative Commons Attribution 3.0 licence. Any further distribution of this work must maintain attribution to the author(s) and the title of the work, journal citation and DOI.
Published under licence by IOP Publishing Ltd

Ga (Sc) atoms [6] and the FM vibronic superexchange interaction coming from disordered and fluctuating JT-distorted Mn^{3+} atoms [7]. Both models assume that the change from A-type AFM to FM ordering is originated by the orbital direction adopted by the Mn^{3+} ion and it is similar for Ga and Sc non-magnetic substitutions, so the atomic e_g orbital would be perturbed in the same way for the two series.

These models contrast with previous x-ray absorption spectroscopy (XAS) studies [8-10]. A XAS study of the $LaMn_{1-x}Ga_xO_3$ series have revealed that the tetragonal distortion of MnO_6 octahedron continuously decreases with the gallium content in such a way that for x>0.5 MnO_6 distortion disappears and becomes regular [8,9], simultaneously to the appearance of long-range FM. Moreover, a XAS study of the isostructural $TbMn_{1-x}Sc_xO_3$ series showed that the MnO_6 octahedra remain tetragonally distorted along the whole dilution range, independently of the Sc content [10].

Here, we have studied the crystallographic structure by x-ray powder diffraction (XRD) and the local structure by XAS at the Mn and Sc K-edges in the $LaMn_{1-x}Sc_xO_3$ series in order to clarify the importance of removing the Jahn-Teller distortion in driving the FM behavior.

2. Experimental details

Powder $LaMn_{1-x}Sc_xO_3$ (x= 0, 0.1, 0.2, 0.3, 0.4, 0.5, 0.6, 0.7, 0.9, 1) samples were synthesized following the same ceramic procedure as previously outlined for $LaMn_{1-x}Ga_xO_3$ [3]. XRD patterns were collected for the whole series in the 2-theta range between 18º and 135º at room temperature by using a D-max Rigaku system with a rotating anode and selecting the Cu Kα radiation. The crystal structures were refined by the Rietveld method using the program FULLPROF [11]

The Mn K-edge XAS spectra were recorded at the BM23 beamline of the European Synchrotron Radiation Facility. Data were recorded at a fixed T ~ 80 K in transmission mode for Sc concentration up to x=0.6 while for higher dilutions fluorescence detection was used. The Sc K-edge XAS measurements were carried out at fixed temperature at the CLAESS beamline of the ALBA synchrotron for Sc concentration x≥0.3 whereas temperature-dependent XAS spectra of the $LaMn_{0.4}Sc_{0.6}O_3$ sample were collected at the XAFS beamline of the Elettra Synchrotron. Data for x>0.4 were recorded in transmission mode while for lower Sc concentration fluorescence detection was used. XANES spectra were normalized to unity edge jump using the Athena software from the Demeter package [12]. The extraction of the χ(k) signals were also performed using Athena program, and R-space EXAFS spectra were obtained by calculating the Fourier Transform (FT) of the $k^2\chi(k)$ signals in the (2.5-14) $Å^{-1}$ k-range. The EXAFS structural analysis was performed using theoretical phases and amplitudes calculated by the FEFF-6 code [13] and fits to the experimental data were carried out in R-space with the Artemis program of the Demeter package [12].

3. Results and conclusions

The XRD results show that the tetragonal distortion of the MO_6 octahedron continuously decreases with the Sc content (figure 1). There are two possibilities that could explain this fact: either both MnO_6 and ScO_6 octahedron are equally distorted, and the magnitude of the correlated distortion decreases with x, or the observed distortion of MO_6 by XRD corresponds to the average of different MnO_6 and ScO_6 octahedra. In figure 1, we have compared the M-O distances from XRD with the weighted addition of the Mn-O and Sc-O distances taken from XRD for the end-member compounds of the series, $LaMnO_3$ and $LaScO_3$. The same comparison was also made with the weighted addition of the Mn-O and Ga-O distances for the $LaMn_{1-x}Ga_xO_3$ series as reported in the inset of figure 1. The agreement is very good, which means that the geometrical orientation of the MnO_6 tetragonal distortion is preserved in the *ab* plane in both, Sc-substituted and Ga-substituted compounds. In the Ga-substituted samples, different MnO_6 and GaO_6 octahedra are deduced by XAS where the JT-distortion of the $Mn^{3+}O_6$ decreases with the Ga substitution and the appearing of FM concurs with the presence of regular $Mn^{3+}O_6$ octahedron (x>0.5). The occurrence of Mn tetragonal distortions, which remain ordered even up to high Sc content, has been also reported for the $TbMn_{1-x}Sc_xO_3$ series [10].

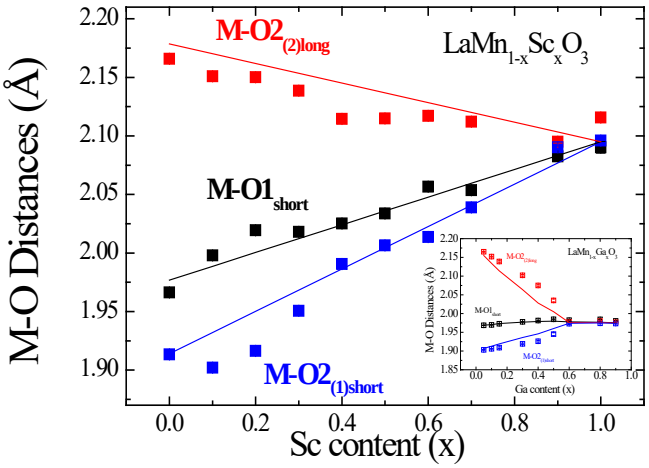

Figure 1. Evolution with the Sc content of the MO_6 octahedron (closed symbols) compared to the weighted addition of the M-O distances of the two end-member $LaMnO_3$ and $LaScO_3$ (lines) from XRD. **Inset:** same comparison for the $LaMn_{1-x}Ga_xO_3$ series.

No edge energy shift is observed between the $LaMn_{1-x}Sc_xO_3$ samples and either the $LaMnO_3$ sample at the Mn K-edge or the $LaScO_3$ sample at the Sc K-edge (figure 2) within the precision of the experiments (0.4 eV). Thus, Mn^{3+} formal valence keeps constant along the dilution.

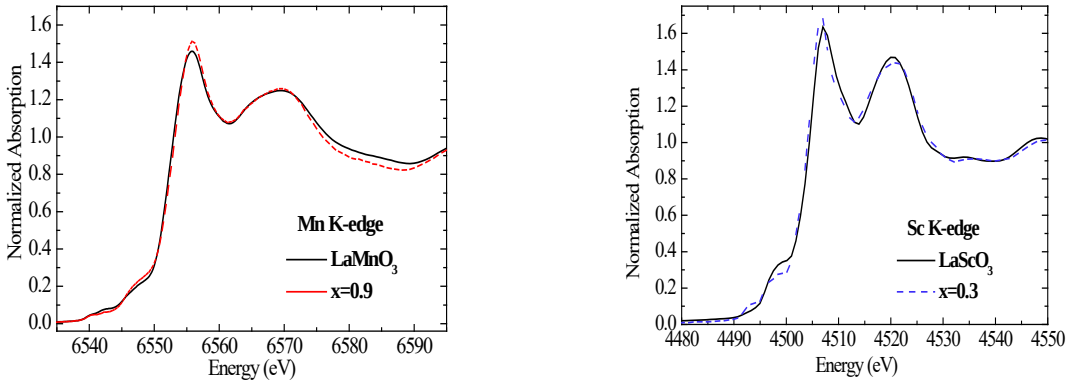

Figure 2. Left. Normalized Mn K-edge XANES spectra of $LaMn_{1-x}Sc_xO_3$ (x=0, 0.9). **Right.** Normalized Sc K-edge XANES spectra of $LaMn_{1-x}Sc_xO_3$ (x=0.3, 1).

Figure 3 shows the modulus of the FT of the k^2-weighted EXAFS signals of selected concentrations of Sc. All samples show a main peak at ~1.5 Å (Mn K-edge) and ~1.6 Å (Sc K-edge) corresponding to the first (Mn-O or Sc-O) coordination shell without phase shift correction. The intensity and shape of this peak is practically independent of the dilution indicating that the oxygen coordination geometry around both, Mn and Sc atoms, remains almost unaltered along the whole series. The structural analysis at the Mn K-edge was performed considering the same shift on the equatorial plane (Mn-$O1_{short}$ and Mn-$O2_{short}$, $delr_1$) and a different one for the apical distances (Mn-$O2_{long}$, $delr_2$) of the MnO_6 octahedron. The relevant structural parameters for the first oxygen coordination shell of all samples are shown in the inset of figure 3(left). The same tetragonal distorted (JT) MnO_6 as in $LaMnO_3$ is found for all Sc substitutions. At the Sc K-edge, we have performed the fits considering the three pairs of Sc-O distances slightly distorted of $LaScO_3$ but they converge to a unique distance. As shown in the inset of figure 3 (right), the same nearly regular ScO_6 octahedron as in $LaScO_3$ is found for all Sc concentrations. The temperature-dependent EXAFS spectra of $LaMn_{0.4}Sc_{0.6}O_3$ at the Mn and Sc K-edges between 80 and 300 K confirm the robustness of MnO_6 tetragonal distortion and the lack of significant static distortion of ScO_6 for $LaMn_{0.4}Sc_{0.6}O_3$ along this temperature range.

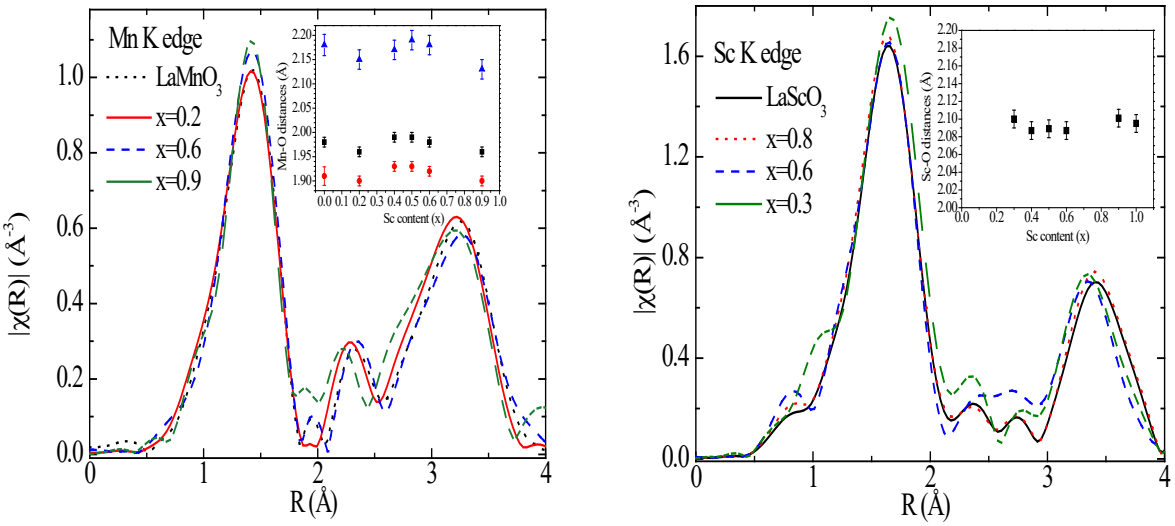

Figure 3. Left. Modulus of the FT at the Mn K-edge for selected $LaMn_{1-x}Sc_xO_3$ samples. **Inset:** Evolution of the fitted Mn-O distances with the Sc content. **Right.** Modulus of the FT at the Sc K-edge for selected $LaMn_{1-x}Sc_xO_3$ samples. **Inset:** Evolution of the fitted Sc-O distances with the Sc content.

The present results show a marked difference in the local structure for $LaMn_{1-x}Ga_xO_3$ and $LaMn_{1-x}Sc_xO_3$. MnO_6 is hardly distorted in an environment composed by regular GaO_6 octahedra whereas this distortion results more feasible when MnO_6 is surrounded by ScO_6 octahedra because of the larger tilts of the ScO_6 octahedron in the orthorhombic *Pbnm* cell. Therefore, the occurrence of the tetragonal distortion of the MnO_6 octahedron strongly depends on the lattice in which Mn atom is allocated. Despite the different structural behaviour found for Ga and Sc substitutions, the magnetic response for $x \geq 0.5$ is similar in both cases. The two proposed models [6,7] to account for the change from A-type AFM to FM cannot be supported by either the present structural study or that in the Ga-substituted samples [8,9] so the Mn-sublattice dilution effect may be the main responsible for the magnetic behaviour of these manganites.

Acknowledgments
Authors acknowledge the financial support from Mineco/FEDER MAT2012-38213-C02-01 and DGA E69 projects. They also thank Alba, ESRF, and Elettra for granting beam time.

References
[1] Ritter C et al. 1997 *Phys. Rev. B* **56** 8902
[2] Hébert S et al. 2002 *Phys. Rev. B* **65** 104420
[3] Blasco J et al. 2002 *Phys. Rev. B* **66** 174431
[4] Goodenough J B et al. 2002 *Sol. State Sci*. **4** 297
[5] Blasco J et al. 2012 *J. Phys.:Condens. Matter* **24** 076006
[6] Farrell J and Ghering G A 2004 *New J. Phys*. **6** 168
[7] Zhou J-S and Goodenough J B 2003 *Phys. Rev. B* **68** 144406
[8] Sánchez M C et al. 2004 *Phys. Rev. B* **69** 184415
[9] Sánchez M C et al. 2006 *Phys. Rev. B* **73** 094416
[10] Cuartero V et al. 2010 *Phys. Rev. B* **81** 224117
[11] Rodríguez-Carvajal J and Roisnel T, http://www-llb.cea.fr/ fullweb/fullprof.98/fp98.htm
[12] Ravel B and Newville M 2005 *J. Synchrotron Radiat*. **12** 537
[13] Rehr J J and Albers R C 2000 *Rev. Mod. Phys*. **72** 621